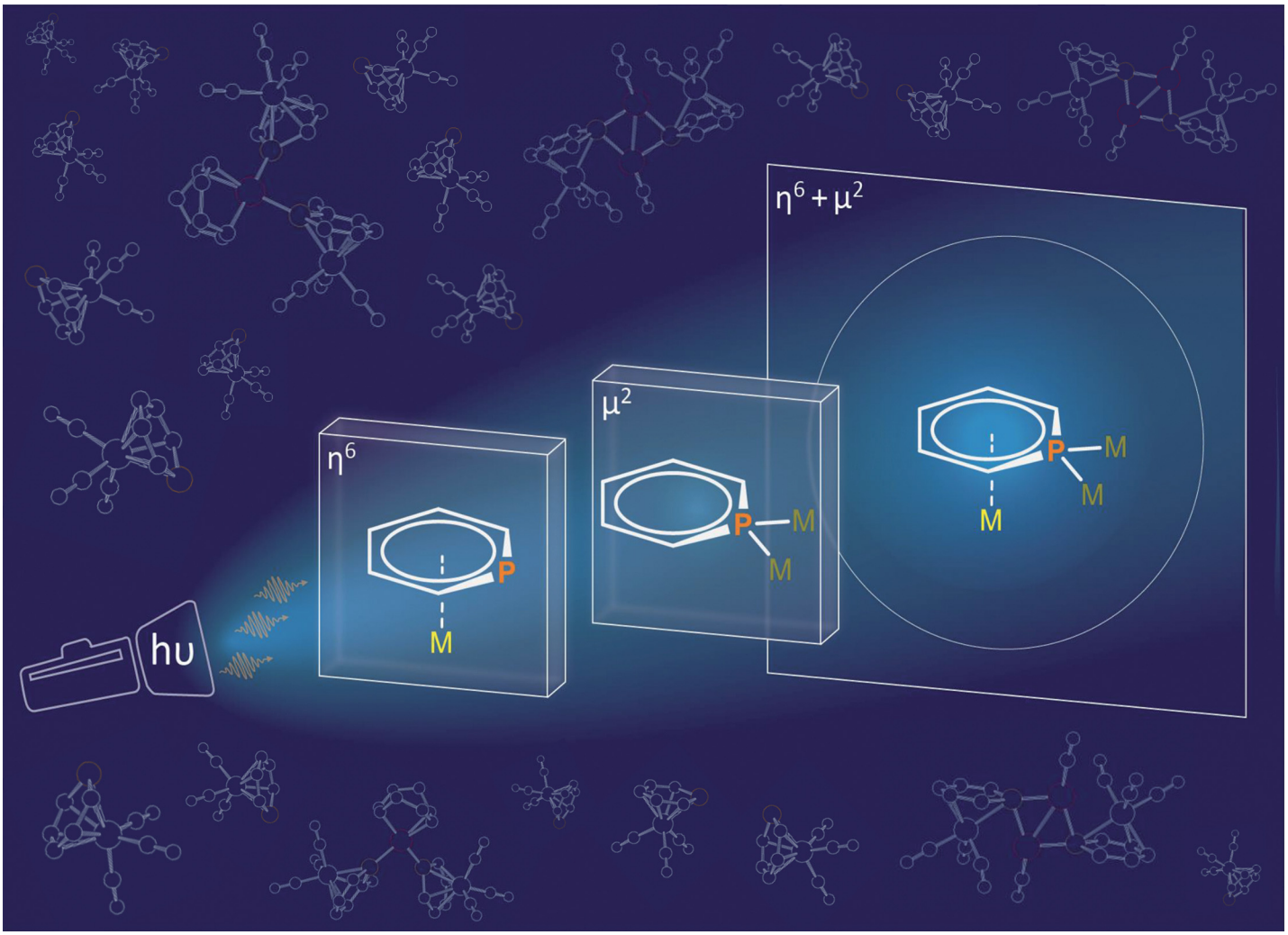

Showcasing research from Professor Christian Müller's laboratory, Institute of Chemistry and Biochemistry, Freie Universität Berlin, Berlin, Germany. Image designed and illustrated by Andrey Petrov and Indira Kaymova.

Highly flexible phosphabenzenes: a missing coordination mode of 2,4,6-triaryl-λ^3-phosphinines

The cover shows the superimposition of two known coordination modes of λ^3-phosphinines to give a hitherto unknown complex, in which the aromatic phosphorus heterocycle acts both as a $6e^-$-π-ligand and, additionally, as a bridging $2e^-$ ligand. The formation of the product is facilitated by UV-light.

As featured in:

See Christian Müller *et al.*, *Chem. Commun.*, 2022, **58**, 6184.

ROYAL SOCIETY OF CHEMISTRY

rsc.li/chemcomm

Registered charity number: 207890

ChemComm

COMMUNICATION

View Article Online
View Journal | View Issue

Cite this: *Chem. Commun.*, 2022, **58**, 6184

Received 30th March 2022,
Accepted 13th April 2022

DOI: 10.1039/d2cc01817a

rsc.li/chemcomm

Highly flexible phosphabenzenes: a missing coordination mode of 2,4,6-triaryl-λ^3-phosphinines†‡

Erlin Yue, §[ab] Andrey Petrov,§[a] Daniel S. Frost, [a] Lea Dettling, [a] Lawrence Conrad,[a] Friedrich Wossidlo,[a] Nathan T. Coles,[a] Manuela Weber[a] and Christian Müller *[a]

The reaction of 2,4,6-triaryl-λ^3-phosphinine-$Cr(CO)_3$-π-complexes with $[Rh(COD)_2]BF_4$ leads to unusual diamagnetic Rh^0-dimers, which contain two phosphinine-π-complexes acting as a bridging $2e^-$-ligand towards the $Rh_2(CO)_2$ core. These compounds represent a missing coordination mode for the aromatic 6-membered phosphorus heterocycle.

In contrast to classical phosphines (PR_3), phosphinines (phosphabenzenes) show rich and diverse coordination chemistry.[1] As ambidentate ligands, these aromatic phosphorus heterocycles can adopt various coordination modes, in which the phosphorus atom and/or the π-system is involved in the interaction with the metal centre (Chart 1).

The fascinating coordination chemistry of phosphinines has been explored extensively during the last two decades, with particular focus on the reactivity of transition metal phosphinine complexes and their application in homogeneous catalysis and materials science.[2]

η^1-Phosphinine complexes (**A**, $2e^-$-donor) are common and are typically formed with transition metals in low oxidation states.[1] This is due to the fact that phosphinines are very good π-acceptors when the coordination occurs *via* the phosphorus atom.[3] Transition metal complexes with phosphinines as bridging ligands are also known (**B**, μ_2-P, $2e^-$-donor).[1] More recently, it has been shown that electron rich phosphinines (**B**, R = O^-, NMe_2) have a high tendency to act as $4e^-$, μ_2-bridging ligands.[4,5] It is also possible to coordinate *via* the P=C double bond (**C**, η^1-P, η^2-PC, $4e^-$-donor).[1] Phosphinine-η^6-complexes (**D**, $6e^-$-donor) are also accessible,[1] usually by addition of sterically demanding substituents, such as *t*-butyl- or Me_3Si-groups in the α-position of the phosphorus heterocycle, which can prevent σ-coordination *via* the phosphorus lone-pair.[6] With electron rich metal centers, coordination with the π-system can also occur in an η^4-fashion (η^2-CC, $4e^-$-donor) to fulfill the $18e^-$ rule.[1]

Examples, in which the η^6-π-complex **D** serves as a $2e^-$ metallo-ligand (**E**, η^6-PC_5, η^1-P, $8e^-$-donor) are surprisingly rare.[7] On the other hand, such bimetallic species may show interesting properties, which could be exploited in more applied research fields. The corresponding coordination compound **F**, in which the metallo-ligand **D** acts as a bridging $2e^-$-donor (η^6-PC_5, μ^2-P) has so far not been reported in the literature. Elschenbroich and co-workers described the related species **G**, in which the $Mn(CO)_3$-η^5-phosphinine complex coordinates to a binuclear $Mn_2(CO)_7$ fragment.[8] In this compound, the phosphorus atom thus serves as a $3e^-$-donor, while all Mn^0-atoms fulfill the 18 electron rule.

Motivated by the lack of information on complexes of type **E**, we started to investigate the electronic properties and the coordination chemistry of the metallo-ligand **D** in more detail and report the first example of the missing coordination mode

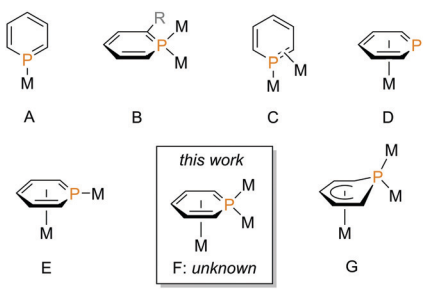

Chart 1 Coordination modes of λ^3,σ^2-phosphinines.

[a] *Freie Universität Berlin, Institute of Chemistry and Biochemistry, Fabeckstr. 34/36, 14195 Berlin, Germany. E-mail: c.mueller@fu-berlin.de*
[b] *Shaanxi Key Laboratory of Chemical Reaction Engineering, Key Laboratory of New Energy & New Functional Materials, College of Chemistry and Chemical Engineering, Yan'an University, Yan'an, Shaanxi 716000, People's Republic of China. E-mail: yueerlin@yau.edu.cn*

† Dedicated to Prof. Christian Bruneau.

‡ Electronic supplementary information (ESI) available. CCDC 2113811–2113814. For ESI and crystallographic data in CIF or other electronic format see DOI: https://doi.org/10.1039/d2cc01817a

§ These authors have contributed equally.

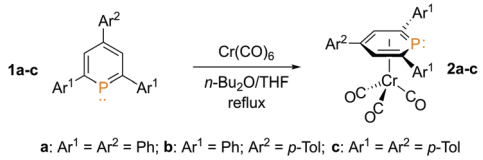

a: $Ar^1 = Ar^2$ = Ph; **b**: Ar^1 = Ph; Ar^2 = *p*-Tol; **c**: $Ar^1 = Ar^2$ = *p*-Tol

Scheme 1 Synthesis of phosphinine-$Cr(CO)_3$-π-complexes **2a–2c**.

η^6-PC_5-μ_2 ($8e^-$) for phosphinines. As arene-η^6-$Cr(CO)_3$ complexes are very common organometallic 18 VE-species, we anticipated that the corresponding phosphinine complexes would be a good starting point for acquiring these species. The π-complex 2,4,6-triphenyl-λ^3-phosphinine-$Cr(CO)_3$ (**2a**) has been reported and structurally characterized by Deberitz and Nöth in 1970.[9] The derivatives **2b**/**c** are easily accessible in moderate yields from 2,4,6-triarylphosphinines **1b**/**c** (Scheme 1). The π-complex **2a** shows a single resonance in the $^{31}P\{^1H\}$ NMR spectrum at δ(ppm) = 6.1 (**2b**: δ(ppm) = 5.5; **2c**: δ(ppm) = 5.1; Fig. S1, S5 and S8, ESI‡).

We were first interested in the electronic properties of the phosphinine-π-complexes. Fig. S53 (ESI‡) illustrates the frontier Kohn–Sham-orbitals of the π-complex $(C_5H_5P)Cr(CO)_3$ (**2a′**) in comparison to the parent phosphinine C_5H_5P. In general, phosphinines are good π-acceptors due to an energetically low-lying LUMO (Fig. S53, ESI‡, left side). On the other hand, they possess weak σ-donor properties, as the phosphorus-lone pair is energetically stabilized (HOMO−2). Interestingly, the corresponding $Cr(CO)_3$-π-complex is both a poorer π-acceptor and an even weaker σ-donor than C_5H_5P (Fig. S53, ESI‡, right side). Thus, it is not surprising that relatively little is known about the coordination chemistry of phosphinine-π-complexes. We anticipated that $Cr(CO)_3$-phosphinine-π-complexes might only be suitable as a metallo-ligand for the coordination to electron rich metal centers.

Because Rh^I complexes of phosphinines are usually straightforward to synthesize, we reacted **2a–c** at room temperature with one equivalent of $[Rh(COD)_2]BF_4$ in CD_2Cl_2. Immediately, a single new species is formed, which shows a doublet resonance in the $^{31}P\{^1H\}$ NMR spectrum at δ(ppm) = 36.8 ($^1J_{P-Rh}$ = 179 Hz, **3a**) when using **2a** as the ligand (**3b**: δ(ppm) = 36.0 ($^1J_{P-Rh}$ = 179 Hz); **3c**: δ(ppm) = 36.2 ($^1J_{P-Rh}$ = 179 Hz); Fig. S11, S16 and S21, ESI‡). When the reaction is performed with a ligand : metal ratio of 2 : 1 (**2a–c**: Rh), one equivalent of **2a–c** remains in solution. Attempts to crystalize the corresponding products **3a–c** were unsuccessful. However, upon substituting the $[BF_4]^-$ counterion of **2c** for $[BAr^F_4]^-$ (Ar^F = $(CF_3)_2C_6H_3$), we were able to isolate the Rh^I complex **3d**, which was characterized crystallographically. The molecular structure of **3d** in the crystal confirms the presence of two $Cr(CO)_3$-phosphinine-π-complexes bound to the $[Rh(COD)]^+$ fragment *via* the phosphorus lone-pair (Fig. 1). To confirm whether the observed structure of **3a–c** was retained in solution, the $^{31}P\{^1H\}$ NMR spectrum of a reaction containing both **2a** and **2b** with $[Rh(COD)_2]BF_4$ in a ratio of 1 : 1 : 1 gave signals for a species with an ABX spin system, indicating the formation of [Rh(**2a**)(**2b**)(COD)]BF_4 (Fig. S26, ESI‡). The spectrum also reveals two doublets and two singlets that correspond to **3a** and **3b**, as well as to free ligands **2a** and **2b** respectively. Based on this NMR experiment, we anticipate that

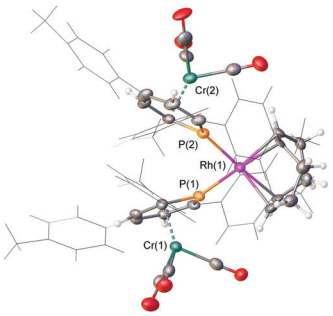

Fig. 1 Molecular structure of **3d** in the crystal. Displacement ellipsoids are shown at the 50% probability level. Counter anion ($[BAr^F_4]^-$) is omitted for clarity. The pendant groups of the metallo-ligands are shown in wire form for clarity. Selected bond lengths (Å) and angles (°): selected bond lengths (Å) and angles (°): P1–Rh1: 2.3072(17); P2–Rh1: 2.2826(17); P2–Rh1–P1: 88.67(6).

two metallo-ligands are coordinated to one Rh^I-center to form **3a–c** which are in a dynamic equilibrium in solution (Scheme 2).

When reaction mixtures containing **3a–c** were left standing, orange crystals formed after several weeks, along with an insoluble precipitate. Much to our surprise, the $^{31}P\{^1H\}$ NMR spectra of the crystals in CD_2Cl_2 show a complex multiplet resonance at around δ(ppm) = 172.0 (Fig. 2b).

The spectra can be simulated as an AA′XX′ spin system, arising from P–P′, Rh–P and Rh–Rh′ interactions (Fig. 2a). From the ^1H–^{103}Rh HMQC NMR spectra the chemical shifts of the Rh atoms were identified at around δ(ppm) = −9245 (Fig. S43, ESI‡). The NMR spectroscopic studies therefore indicate that a symmetrical dimeric P_2Rh_2 species should be present in solution. Single crystals suitable for X-ray diffraction were obtained for all three new species **4a–c** and the molecular structure of **4b** is depicted in Fig. 3.

The crystallographic characterization of **4b** reveals the missing η^6-PC_5, μ^2-P coordination mode, in which the phosphinine-π-complex acts as a bridging $2e^-$ ligand and forms a fully planar dimeric P_2Rh_2 species with C_i geometry and an anti-arrangement of the two phosphinine-$Cr(CO)_3$ metallo-ligands (Chart 1). The

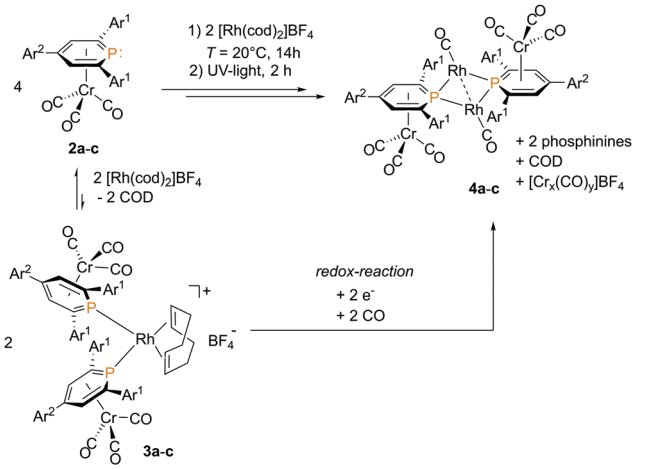

Scheme 2 Synthesis of Rh^I complexes **3a–c** and Rh^0-complexes **4a–c**.

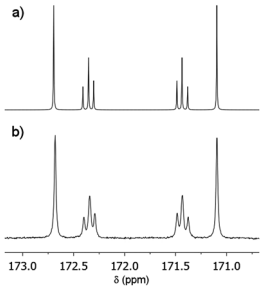

Fig. 2 Simulated (a, AA′XX′) and measured (b) $^{31}P\{^{1}H\}$ NMR spectrum of **4a**.

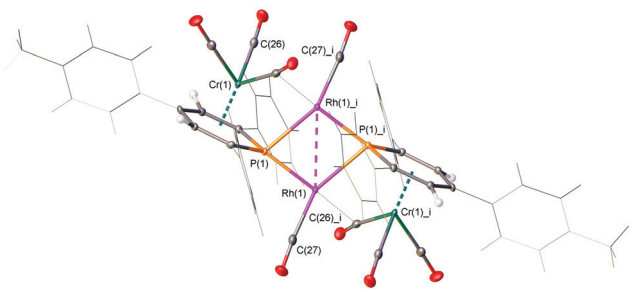

Fig. 3 Molecular structure of **4b** in the crystal. Displacement ellipsoids are shown at the 50% probability level. The pendant aryl-groups of the metallo-ligands are shown in wire form for clarity. Selected bond lengths (Å) and angles (°): P(1)–Rh(1): 2.1947(6); P(1)–Rh(1):_i: 2.3695(6); Rh(1)–Rh(1)_i: 2.8675(4); P(1)–Cr(1): 2.5214(7). Rh(1)–P(1)–Rh(1)_i: 77.743(18); P(1)–Rh(1)–P(1)_i: 102.260(19).

P(1)–Rh(1)–P(1)_1 and Rh(1)–P(1)–Rh(1)_i angles are 102.260(19)° and 77.743(18)°, respectively. The distance between the two Rh-atoms (2.8675(4) Å) indicates an interaction between the two Rh^0 centers, which is in line with the presence of an overall diamagnetic species (Fig. 2 and *vide infra*).[10,11] One CO-ligand of each $Cr(CO)_3$-fragment is semi-bridging and shows short contacts for C(26)–Rh(1)_i and C(26)_i–Rh(1). The crystallographic characterization of **4a** and **4c** show similar results (Fig. S50 and S52, ESI‡). However, the most striking feature of **4a–c** is the fact that two Rh^0 centres are obtained, even though the rhodium atom in the precursor used was in the +1 oxidation state.

To explain the formation of **4a–c**, a redox reaction between the Cr(0)- and Rh(I)-species within **3a–c** has to be presumed. In fact, it is known that arene–$Cr(CO)_3$ complexes undergo photooxidation under UV-light and decompose in solution to give benzene, CO and a grey-green solid. It has further been shown, for instance, that the photolysis of $(\eta^6\text{-}C_6Et_6)Cr(CO)_3$ leads to photo-fragmentation prior to one-electron oxidation.[12] As we also observed decomposition of the π-complex **2a** under UV-light (Fig. S4, ESI‡), we anticipated that the formation of **4a–c** from **3a–c** might also be accelerated by light (Scheme 2). Gratifyingly, the photolysis of a solution of **3a–c** in CD_2Cl_2 with UV-light (λ = 365 nm) leads within 2 h to **4a–c**, an insoluble solid and a signal for the η^1-phosphinine-Rh^I complex in the $^{31}P\{^{1}H\}$ NMR spectrum (Fig. S4 and S47, ESI‡). The partial decomposition of **3a–c** might facilitate the necessary redox reaction and the acquisition of an equivalent of carbon monoxide. Indeed, a survey of the precipitate by XPS analysis reveals the presence of chromium in the oxidation state +3 (Fig. S48, ESI‡). Moreover, the UV-vis spectra of the products consist of intense bands at λ_{max} = 260 nm and less intense broad bands at λ_{max} = 350 nm (Fig. S35, S39 and S44, ESI‡), which can be attributed to MLCT transitions (Fig. S58–S61, ESI‡), confirmed by TDDFT studies. The desired products were obtained in reproducible yields of up to 30%. A similar process has also been observed for bis-η^1-monophosphaferrocene palladium complexes.[13] Similarly, compounds **4a–c** can only be formed in a maximum theoretical yield of 50%. Furthermore, the solid state structures of **4a–c** are perfectly in line with the $^{31}P\{^{1}H\}$ NMR spectra (Fig. 2) of a diamagnetic species in solution. Preliminary CV studies of **4c** (Fig. S45 and S46, ESI‡) show that the complex undergoes an irreversible reduction at E_{red} = −1.59 V (100 mV s^{-1}, *vs.* $Fc^{*+/0}$) upon scanning cathodically in THF. The return oxidation wave appears at E_{ox} = −0.78 V. The cyclic voltammogram of **2c** shows the same processes but with a shift to the cathodic region (Fig. S45, ESI,‡ E_{red} = −1.98 V; E_{ox} = −0.99 V), due to the energetically destabilized LUMO compared to **4c**. Similarities in the shapes of the cyclic voltammograms of **2c** and **4c** (Fig. S45, ESI‡) suggest that only the phosphinine-$Cr(CO)_3$-fragment in complex **4c** was electrochemically active. No other processes were observed upon scanning anodically.

In order to investigate the bonding situation in the Rh-dimer, DFT studies at the ωB97X-D3/def2-TZVP[14] level were performed on the truncated model compounds **2a′** and **4a′** (Ar^1/Ar^2 substituted by H) and on the non-truncated molecule of **4a**. The σ-character of the different P–Rh bonds in **4a′** is illustrated by the HOMO−1 and HOMO−4 (Table S5, ESI‡) as well as by an intrinsic bond orbital (IBO) (Table S2, ESI‡, IBO1a/b, IBO2a/b) and a natural bond orbital (NBO) analysis (Table S3, ESI‡).[15,16] The IBO in Fig. 4a seems to arise from the P1–Rh1 coordination of the lone pair at the phosphorus atom of the phosphinine–$Cr(CO)_3$ complex **2a′** (Table S2, ESI‡). Fig. 4b supports the suggested Rh–Rh interaction, which are also apparent in the HOMO−8, HOMO−13 and HOMO−14 (Table S5, ESI‡). The two significantly distinct P–Rh bond lengths in the rhomboidal Rh_2P_2 core can be rationalized by the additional π-character of the shortened P1–Rh1 bond. The shape of the IBO in Fig. 4c already indicates the presence of back donation from Rh-centered d-orbitals to the phosphorus center. The analysis of the bonding in **4a′** by means of NBO-DFT calculations revealed that the Rh-center donates electron density into two equivalent σ*(P–C) orbitals of the phosphinine ring (Table S4a, ESI‡). The energetic stabilization by the donor–acceptor interactions is $\Sigma E(2)$ = 14.22 kcal mol^{-1} and is visualized in Fig. 4d for the donation into the σ*(P(1)–C(3)) orbital. The shape of LUMO+6 of **2a′** seems ideal to act as an acceptor orbital for these interactions (Table S4b, ESI‡). The orbital energy in comparison to the LUMO is arguably high (E_{LUMO} = 0.436 eV; E_{LUMO+6} = 2.472 eV; $\Delta E_{((LUMO+6)-LUMO)}$ = 2.036 eV), however the σ*(P–C) orbitals contribute 19.9% to the overall orbital composition of the LUMO+6 and justify the assignment. Stabilizing interactions with antibonding P–C-orbitals of phosphinines and their influence on bond lengths have been previously described by Le Floch and by us.[17]

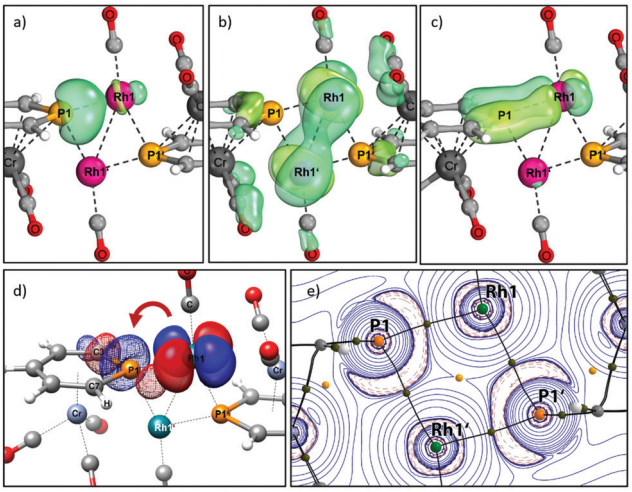

Fig. 4 IBOs of **4a**′ involving (a) a σ-bond between the P1 and the Rh1 atom, (b) Rh–Rh interactions and (c) back donation between P1–Rh1 (IBOs encompass 70% of the density of the orbital electrons); (d) NBO plots of a donor–acceptor interaction between a σ*(P–C) orbital and Rh-centered d-orbital (isosurface value at ±0.08 a.u.); (e) AIM (Bader) analysis (bond critical points: brown, ring critical points: orange) with Laplacian of the electron density plotted in plane of the Rh_2P_2 ring.

A Wiberg bond index (WBI) analysis[18] for **4a**′ provided values of 0.63 and 0.31 for the P1–Rh1 and P1–Rh1′ bonds, respectively, and a WBI of 0.11 for the Rh–Rh interaction. Almost identical values were found for **4a**. The AIM analysis[19] (Fig. 4e and Fig. S54, S55, ESI‡) shows no BCP for the Rh–Rh interaction, but instead a ring critical point (RCP) at the ring center of **4a** and **4a**′. In summary, the calculations suggest that the Rh–Rh interaction is rather weak. The topological properties at BCPs and RCPs for selected bonds and rings in **4a** and **4a**′ are summarized in Table S7 (ESI‡) and complete molecular graphs are shown in Fig. S56 and S57 (ESI‡).

The values of ρ_{BCP} for the P1–Rh1 and P1′–Rh1′ bonds in **4a** are at the low end for shared interactions but significantly larger than those associated with a closed-shell interaction.[20] The smaller values of ρ_{BCP} found for the longer P1–Rh1′ and P1′–Rh1 bonds reflect the rhomboidal geometry of the dimer. The negative energy densities H_{BCP} of the ring bonds are typical for covalent contributions.[21] The full molecular graph of **4a** reveals additional stabilizing closed-shell intramolecular interactions (shown as dashed lines) for i.a. CH···O and Rh···HC, as well as a BCP between Rh1′ and C25 of the carbonyl group that bridges to the $Cr(CO)_3$-fragment (*vide supra*). Notably several other occupied molecular orbitals (HOMO−1, HOMO−4, HOMO−8, HOMO−12, Table S5, ESI‡) and IBOs suggest interactions between Cr1 and Rh1′ (and Cr1′ and Rh1). The WBI analysis on the other hand gave only values of 0.10 for the Rh–Cr interaction and no bond critical points.

In summary, we have synthesized a complex containing the previously unknown η^6-PC_5, μ^2-P coordination mode of a phosphinine, in which the aromatic phosphorus heterocycle acts both as a $6e^-$-π-ligand towards a $Cr(CO)_3$-fragment and, additionally, as a bridging $2e^-$ ligand towards a rather rare $Rh^0{}_2(CO)_2$-core. These diamagnetic coordination compounds were characterized both by NMR spectroscopy and X-ray diffractometry. DFT calculations gave insight into the bonding situation within the phosphinine-bridged Rh_2-dimer.

E. Y. and C. M. are grateful for financial support provided by the Sino-German (CSC-DAAD) Postdoc Scholarship Program (57251553). The authors thank the Scientific Computing Service of Freie Universität Berlin for the use of high-performance computing resources as well as M. W. G. M. Verhoeven (Eindhoven University of Technology, The Netherlands) and Dr. G. J. A. Mannie (SPECS Surface Nano Analysis GmbH, Berlin) for their kind support and help with the XPS analysis.

Conflicts of interest

There are no conflicts to declare.

Notes and references

1 (*a*) P. Le Floch and F. Mathey, *Coord. Chem. Rev.*, 1998, **178-180**, 771; (*b*) N. Mézailles, F. Mathey and P. Le Floch, *Prog. Inorg. Chem.*, 2001, 455; (*c*) P. Le Floch, *Coord. Chem. Rev.*, 2006, **250**, 627; (*d*) N. T. Coles, A. S. Abels, J. Leitl, R. Wolf, H. Grützmacher and C. Müller, *Coord. Chem. Rev.*, 2021, **432**, 213729.
2 (*a*) C. Müller and D. Vogt, *Dalton Trans.*, 2007, 5505; (*b*) P. Roesch, J. Nitsch, M. Lutz, J. Wiecko, A. Steffen and C. Müller, *Inorg. Chem.*, 2014, **53**, 9855.
3 P. D. Burrow, A. J. Ashe III, D. J. Bellville and K. D. Jordan, *J. Am. Chem. Soc.*, 1982, **104**, 425.
4 Y. Hou, Z. Li, Y. Li, P. Liu, C. Y. Su, F. Puschmann and H. Grützmacher, *Chem. Sci.*, 2019, **10**, 3168.
5 S. Giese, K. Klimov, A. Mikehászi, Z. Kelemen, D. S. Frost, S. Steinhauer, P. Müller, L. Nyulászi and C. Müller, *Angew. Chem., Int. Ed.*, 2021, **60**, 3581.
6 M. Doux, L. Ricard, F. Mathey, P. Le Floch and N. Mézailles, *Eur. J. Inorg. Chem.*, 2003, 687.
7 P. A. Cleaves and S. M. Mansell, *Organometallics*, 2019, **38**, 1595.
8 C. Elschenbroich, J. Six and K. Harms, *Chem. Commun.*, 2006, 3429.
9 (*a*) J. Deberitz and H. Nöth, *Chem. Ber.*, 1970, **103**, 2541; (*b*) H. Vahrenkamp and H. Nöth, *Chem. Ber.*, 1972, **105**, 1148.
10 For paramagnetic Rh^0 complexes see for example: B. de Bruin and D. G. H. Hetterscheid, *Eur. J. Inorg. Chem.*, 2007, 211.
11 A. F. Heyduk, A. M. Macintosh and D. G. Nocera, *J. Am. Chem. Soc.*, 1999, **121**, 5023.
12 (*a*) A. Gilbert and J. M. Kelly, *Z. Naturforsch.*, 1976, **31b**, 1091; (*b*) R. G. Compton, R. Barghout, J. C. Eklund, A. C. Fisher, S. G. Davies, M. R. Metzler, A. M. Bond, R. Colton and J. N. Walter, *J. Chem. Soc., Dalton Trans.*, 1993, 3641.
13 X. Sava, L. Ricard, F. Mathey and P. Le Floch, *Chem. – Eur. J.*, 2001, **7**, 3159.
14 (*a*) S. Grimme, J. Antony, S. Ehrlich and H. Krieg, *J. Chem. Phys.*, 2010, **132**, 154104; (*b*) F. Weigend and R. Ahlrichs, *Phys. Chem. Chem. Phys.*, 2005, **7**, 3297; (*c*) J.-D. Chai and M. Head-Gordon, *Phys. Chem. Chem. Phys.*, 2008, **10**, 6615.
15 G. Knizia, *J. Chem. Theory Comput.*, 2013, **9**, 4834.
16 J. P. Foster and F. Weinhold, *J. Am. Chem. Soc.*, 1980, **102**, 7211.
17 (*a*) A. Moores, T. Cantat, L. Ricard, N. Mézailles and P. Le Floch, *New J. Chem.*, 2007, **31**, 1493; (*b*) F. Wossidlo, D. S. Frost, J. Lin, N. T. Coles, K. Klimov, M. Weber, T. Böttcher and C. Müller, *Chem. – Eur. J.*, 2021, **27**, 12788.
18 K. B. Wiberg, *Tetrahedron*, 1968, **24**, 1083.
19 R. F. W. Bader and Acc Chem, *Res.*, 1985, **18**, 9.
20 (*a*) P. Macchi and A. Sironi, *Coord. Chem. Rev.*, 2003, **238-239**, 383; (*b*) E. Espinosa, I. Alkorta, J. Elguero and E. Molins, *J. Chem. Phys.*, 2002, **117**, 5529.
21 (*a*) D. Cremer and E. Kraka, *Angew. Chem., Int. Ed.*, 1984, **23**, 627; (*b*) F. Cortés-Guzmán and R. Bader, *Coord. Chem. Rev.*, 2005, **249**, 633.